THE INVESTIGATION OF A DUCTILE FRACTURE OF A LOW ALLOY STEEL

C.Q. ZHENG* and J.C. RADON+

The relation of two parameters, J-integral and CTOD, characterising fracture toughness is analysed and the results applied in the evaluation of the toughness of a low alloy steel used in the construction of North Sea Oil platforms.

It is shown that the value of the parameter M in the equation $J = M \sigma_y \delta$ decreases with temperature, but is not substantially influenced by the ratio a/W. Suitable expressions to estimate the value of M are discussed.

ANALYSIS OF THE J-INTEGRAL AND CTOD RELATIONSHIP

The characterisation of the fracture process by means of the J-integral and the crack tip opening displacement CTOD is well established. Suitable solutions exist for linear-elastic (using K-factor) and rigid-plastic materials.

However, only approximations are at present available for strain hardening elastic-plastic materials. The solutions reported in the literature so far were normally arrived at by using the linear-elastic approach together with appropriate numerical correction factors. In the present paper, the experimental evaluation of some mechanical properties (J_{1c}, COD) obtained on a low alloy steel BS4360-50D is compared with investigations using other methods on steels of similar compositions (1a). There is a considerable shortage of information on the correlation of fracture toughness properties with the micromechanics processes controlling ductile fractures. On the micromechanics scale fracture occurs by the initiation, growth and coalescence of voids (1b) formed at inclusions and second phase particles. Unfortunately, the relationship between these microscopic processes and the macroscopic behaviour of the material is not well understood.

In the following section on the deformation of a rigid-plastic and elastic-plastic material the process involving static homogeneous strain hardening is considered (1b). Cyclic hardening and fatigue crack propagation are described elsewhere (1c, 1d).

* Northwestern Polytechnic University, Xian, The People's Republic of China.

+ Department of Mechanical Engineering, Imperial College of Science and Technology, London, SW2 2BX.

Rigid Plasticity

In Figure 1, AOB is the opening displacement of the crack tip, CTOD, which increases with the increasing load. At the crack tip $\sigma_{yy} = \sigma$. According to the definition of J-integral

$$J = \int_{GFEDC} \left(W\,dy - \bar{T}\,\frac{\partial \bar{u}}{\partial x}\,ds\right) \tag{1.1}$$

$$= \int_{AOB} \left(W\,dy - \bar{T}\,\frac{\partial \bar{u}}{\partial x}\,ds\right)$$

$$= \int_{AOB} W_p\,dy$$

where W_p = plastic strain energy density. Along the line AOB, $\bar{T} = 0$. Assuming that:

The effective stress $\bar{\sigma} = \alpha\,(\bar{\varepsilon}_p)^n$ (1.2)

where: $\bar{\sigma} = \sqrt{\tfrac{1}{2}\left[(\sigma_1 - \sigma_2)^2 + (\sigma_2 - \sigma_3)^2 + (\sigma_3 - \sigma_1)^2\right]}$ (1.3)

and the effective plastic strain is

$$\bar{\varepsilon}_p = \frac{2}{3}\sqrt{\tfrac{1}{2}\left[(\varepsilon_{p.1} - \varepsilon_{p.2})^2 + (\varepsilon_{p.2} - \varepsilon_{p.3})^2 + (\varepsilon_{p.3} - \varepsilon_{p.1})^2\right]} \tag{1,4}$$

It is usual to express the strain energy density as follows:

$$dW_p = \bar{\sigma}\,d\bar{\varepsilon}_p \tag{1.5}$$

Therefore:

$$W_p = \int \bar{\sigma}\,d\bar{\varepsilon}_p \tag{1.6}$$

$$= \int \alpha\,(\bar{\varepsilon}_p)^n\,d\bar{\varepsilon}_p = \frac{\alpha}{1+n}\,(\bar{\varepsilon}_p)^{n+1} = \frac{1}{n+1}\,\bar{\sigma}\,\bar{\varepsilon}_p$$

and:

$$J = \frac{1}{n+1}\int_{AOB} \bar{\sigma}\,\bar{\varepsilon}_p\,dy \tag{1.7}$$

A free surface near the notch root (Figures 1 and 2) should be noted. As shown in Fig. 2 the three principal stresses are :

σ_{tt}, σ_{nn} and σ_{zz},

where $\sigma_{nn} = 0$.

(a) For plane strain conditions:

$$\sigma_{zz} = \tfrac{1}{2}\sigma_{tt}\ ,\ \varepsilon_{zz} = 0\ ,\ \varepsilon_{tt} = -\varepsilon_{nn}$$

therefore: $\bar{\sigma} = \frac{\sqrt{3}}{2}\,\sigma_{tt}$ and $\bar{\varepsilon}_p = \frac{2\sqrt{3}}{3}\,\varepsilon_{tt}$ (1.8)

(b) For plane stress conditions:

$$\sigma_{zz} = 0\ ,\ \varepsilon_{zz} = \varepsilon_{nn} = -\tfrac{1}{2}\varepsilon_{tt}$$

therefore: $\bar{\sigma} = \sigma_{tt}$ and $\bar{\varepsilon}_p = \varepsilon_{tt}$ (1.9)

In both plane strain and plane stress conditions, along the free surface of the notch root:

$$\bar{\sigma}\,\bar{\varepsilon}_p = \sigma_{tt}\,\varepsilon_{tt} \tag{1.10}$$

This relation applies to any free surface of arbitrary shape. Therefore:

$$J = \frac{1}{n+1}\int_{AOB} \bar{\sigma}\,\bar{\varepsilon}_p\,dy = \frac{1}{n+1}\int_{AOB} \sigma_{yy}\,\varepsilon_{yy}\,dy = \frac{1}{1+n}\,\sigma\,\delta_p \tag{1.11}$$

where $\sigma = \sigma_{yy}$ and $\delta_p = \int \varepsilon_{yy}\,dy$, is the plastic part of the CTOD. Neither a specific shape of the plastic zone, nor the distribution of stress were taken into account in equation 1.11.

Elasticity-Plasticity

Strain energy, U, consists of elastic part U_e and plastic part U_p, as follows:

$$U = U_e + U_p \tag{2.1}$$

Similarly, it is convenient to express J as J_e plus J_p and δ as δ_e plus δ_p. Using eq, (2.1), the expression for J-integral is:

$$J = -\frac{1}{B}\left(\frac{\partial U}{\partial a}\right)_\Delta$$

$$= -\frac{1}{B}\left(\frac{\partial U_{el}}{\partial a}\right)_\Delta - \frac{1}{B}\left(\frac{\partial U_p}{\partial a}\right)_\Delta \tag{2.2}$$

$$= G + \frac{1}{n+1}\,\sigma\,\delta_p$$

This equation has also been derived by Chen et al (2), as described later. In the elastic range:

$$J = G \tag{2.3}$$

In the large plastic strain range:

$$J \simeq \frac{1}{1+n}\,\sigma\,\delta_p \tag{2.4}$$

At the critical point when σ increases to fracture, $\sigma = \sigma_f$ (fracture stress):

$$J_c \simeq \frac{1}{1+n}\,\sigma_f\,\delta_c = \frac{1}{1+n}\left(\frac{\sigma_f}{\sigma_y}\right)\sigma_y\,\delta_c \tag{2.5}$$

$$\frac{J_c}{\sigma_y\,\delta_c} = \frac{1}{1+n}\,\frac{\sigma_f}{\sigma_y}$$

Thus J_c is dependent on the strain hardening exponent n and on the ratio of fracture stress and yield stress σ_f/σ_y.

The direct proportionality of the J-integral and CTOD, (δ), as discussed above, is well known. A simple relationship describing this proportionality may be expressed conveniently in the form:

$$J = M\,\sigma_y\,\delta \tag{2.6}$$

where M is an empirical coefficient, which, according to analytical and experimental investigations, lies between 1 and 2. It will be shown in the following paragraphs that these limits are highly approximate. Large discrepancies between these analytical and experimental values of M reported in the literature advocate the need for better research methods than those presently used. The value of the yield stress, σ_y, corresponding to the strain rate and the temperature applied in the testing process are particularly relevant. Other, more complicated relations than eqn. 2.6 may be found in the literature. For example, Chen et al (2) derived the expression (see eqn. 2.2).

$$J = G + \frac{1}{1+n}\,\sigma\,\delta_p \tag{2.7}$$

for power-law hardening materials, where σ denotes the value of stress σ_{yy} at the root of the blunted crack tip, and δ_p is the plastic part of CTOD at the crack initiation. In eqn. 2.7, n is the static strain hardening exponent. The discrete value of the yield stress in eqn. 3.1 is replaced here by σ which represents σ_f = flow stress at fracture. Equation 2.7 may be rearranged as:

$$J_c = G_c + \frac{1}{1+n}\,\sigma_f\,(\delta_p)_c \tag{2.8}$$

and considering only plastic deformation we obtain

$$J_{pc} = \frac{1}{1+n}\,\sigma_f\,(\delta_p)_c \tag{2.9}$$

where J_{pc} denotes the plastic part of J_c. The terms G_c (or J_{ec}) is the elastic part of J_c and, similarly, $(\delta_e)_c$ is the elastic part of CTOD.

For high toughness materials Eqn. 2.9 will change to:

$$\frac{1}{1+n}\,\sigma_f\,(\delta_p)_c \gg G_c \tag{2.10}$$

In this case:

$$J_c \simeq \frac{1}{1+n}\,\sigma_f\,(\delta_p)_c \tag{2.11}$$

or,

$$J_c \simeq \frac{1}{1+n}\,\frac{\sigma_f}{\sigma_y}\,\sigma_y\,(\delta_p)_c \tag{2.12}$$

Consequently, using Eqn. 2.6

$$M \simeq \frac{1}{1+n}\,\frac{\sigma_f}{\sigma_y} \tag{2.13}$$

Experimental

According to Bridgman (3), the flow stress at fracture, σ_f, can be calculated from:

$$\frac{\sigma_f}{\sigma_M} = \frac{1}{(1 + 2R/a)\ \ln\ (1 + a/2R} \tag{3.1}$$

where $\sigma_M = P_f/(\Pi a^2)$ = average tension in the neck of the specimen at fracture, Fig. 3. The values experimentally determined (1) for BS4360-50D steel (Table 1) are:

P_σ = 40.11 kN (Figure 1)

σ_y = 383 MPa

R = 3.30 mm (Figure 2)

a = 3.32 mm (Figure 2)

and applying eqn. 3.1 we obtain: σ_f = 951 MPa. These results were obtained using cylindrical specimens, 11.28 mm in diameter, as described in (1a). Other tensile properties are shown in Table 4.

Table 2 shows the values of M calculated from eqn. 2.13, together with the relevant experiment results. Using n = 0.27, which corresponds to the condition of large strain immediately after necking (1), we obtain:

$$M = 1.96 \tag{3.2}$$

for the steel 50D at room temperature, and this is not very different from the values quoted in Table 2. Chen (6) also considered a hyperbolic rather than circular profile of the necked section, Fig. 4. In this case, the relevant equation differs only slightly from eqn. 3.1. It can be shown that it takes the form:

$$\frac{\sigma_f}{\sigma_M} = \frac{2}{1 + (1 + R/a)\ \ln\ (1 + a/R)} \tag{3.3}$$

In the present work, the necked profile was approximated to hyperbolic, parabolic and circular shapes. For the same steel, no substantial difference was noted and the detailed analysis of the necked shape indicated only a very small deviation of the relevant results (less than 1.5%). However, the strain ε_p in the center of a tensile specimen may not correspond with that measured close to the blunted crack tip of a three-point bend specimen.

It is interesting to note that Castro (4) obtained a mean experimental value of M equal to 1.80. Although his results were evaluated at -10°C, it is unlikely that M would substantially change within the temperature range of 30°C. Pisarski (5) reported experimental values:

$$M = 2.25 \tag{3.4}$$

which are 20% higher than Castro's results. Nevertheless, both results based on standard instrumentation agree reasonably well with the predicted values. Note that a mean value of $M \simeq 2.25$ was estimated from Figure 8 and Figure 9 in Ref. (5) for $\Delta a = 0 \div 1.6$ mm, and the limits for $M \simeq 2.1 \div 2.4$; an exact M value has not been specified in this work.

Another equation originally developed by Lautridou et al. (9) is:

$$M = \frac{1}{0.54\ (1 + n)} \left(\frac{2}{\sqrt{3}}\ (1 + \nu)\ (1 + n)\ \frac{\sigma_y}{nE}\right)^{-n} \tag{3.5}$$

Lautridou reported the calculated values close to the experimental results on A508 steel. Equations 2.13 and 3.5 are compared with the experimental data (10,5,9,4) in Table 3; it will be noted that the value of M calculated by formula 2.13 is in good agreement with the experimental results, while in eqn. 3.5 the difference is substantial. Hence the form of the eqn. 3.5 may require further adjustment, such as a suitable reduction of the size factor.

The reported experimental results, σ_f/σ_y vs σ_y and n vs σ_y are presented in Figure 5 for medium strength steels ($\sigma_y \simeq 400 \div 1000$ MPa). The value of M estimated using eqn. 2.13 lies between 1.5 to 2.6 and this coincides well with a number of experimental values reported in the literature. Some recent results from Refs. (4a, 4b) and (10) have been replotted in Fig. 6. The data for the low-alloy steel BS4360-50D, obtained on three-point bend specimens are particularly relevant here.

It has been suggested (4) and (10) that the value of M may decrease with decreasing temperature, Figure 6. It will be noted that the curves are similar in shape, although they represent three different steels. With the increasing temperature, the value of M initially increases very quickly. This trend is related to the quality of the material and the gradual levelling at higher temperatures is probably due to the proximity of the transition temperature. The values of M at high temperatures are very similar to those of other steels. Experiments at very low temperatures, where M is expected to decrease substantially, are now in preparation and additional tests on other structural steels would be of particular interest.

The influence of the geometrical size of the test piece on the value of M has also been investigated. It was reported (10) that there is a

distinct effect of specimen dimensions on the J-CTOD relationship for materials such as BS4360-50D steel, according to the equation:

$$M = 3.32\ (a/W - (a/W)^2)^{\frac{1}{2}} \tag{3.6}$$

and at a/W = 0.5, the value of M may reach the maximum, $M_{max} = 1.66$. However, according to the subsequent experimental results (4) it was suggested that at least for BS4360-50D steel, M was insensitive to the value of a/W. Hence it seems possible that results in (4) and (10) should be reanalysed. As indicated, the approximate expression for the factor M yields correct values within ± 10% for a/W between 0.4 and 0.6 and this is adequate for many practical applications. Beyond this range, the margin of error may be unacceptably large.

Using eqn. 3.6, the value of M varies between 1.626 and 1.66; this is only a 2% difference in the value of a/W for the whole range of 0.4 to 0.6. Thus (4) and (10) support the evidence that there is no direct influence of a/W on the value of M. Again, further tests using widely different geometries would be helpful.

It is expected that some other properties, such as E, and also σ_y, n and the strain rate may influence the value of M. A relationship including these factors may well be more complicated than, for example, that incorporated in the eqn. 3.5. The effect of the strain hardening exponent, as a function of loading history is likely to lead to higher M values; this investigation is now in progress. On the other hand, with the increasing strain or loading rate the value of M will probably decrease. Similarly, the general trend for steels is that as the yield increases, the M value decreases.

CONCLUSIONS

It is suggested that the relationship of the J-integral and CTOD requires further investigation. Some convenient estimates should be used in the meantime. In summary, for the low-alloy steel BS4360-50D:

1. Evidence is presented showing that the experimental results now available and the eqns. 2.2 and 3.2 give a good general estimat of the J-integral. Also this J-value agrees well with the experimental results recently reported in the literature.

2. Bridgman's functions may be used to closely describe the neck profile in the ductile fracture of a tensile specimen. These functions would not influence parameters R, σ_f and M.

3. On the basis of the data at present available, it seems that the value of M decreases with decreasing temperature. Between 200°K and 300°K, M is nearly constant and for BS4360-50D steel is 1.80.

4. In the range of $0.4 \lesssim a/W \lesssim 0.6$, there is practically no influence of a/W on the paramater M. However, outside this range the value of M may be suspect and the results should be used with care.

TABLE 1

Chemical Composition (Weight) of BS4360-50D Steel

Element	C	Si	Mn	Ni	Cr	Mo	P	S	Cu	Nb	Al
%	0.180	0.36	1.40	0.095	0.11	0.020	0.018	0.003	0.16	0.039	0.035

TABLE 2

The Values of M

Hardening Exponent n	M from Equations (8) and (9)	M from Equations (8) and (11)	M experimental
0.174	2.12	2.15	1.80 [4]
0.22	2.04	2.08	2.25 [5]
0.27	1.96	2.00	-

TABLE 3

Estimated and Experimental Values of M

Steel	Hardening Exponent n	σ_y (MPa)	M experimental	M from Equation 8)	M from Equation 12)
BS4360-50D	0.27	383	1.80 [4] to 2.26 [5]	1.96	4.74
En32B	0.28	290	2.52 [9]	2.73	5.29
En32	0.289	275	2.60 [10]	2.72	5.60
	0.221	275	2.60 [10]	2.87	4.09

REFERENCES

(1a) ZHENG, C Q and RADON, J C. 'Basic tensile properties of a low-alloy steel BS4360-50D, in Proc. Int. Conf. on Fracture Mechanics Technology Applied to Material Evaluation and Structure Design, Melbourne, Australia. Den Hague, G.C. SIH, W E RYAN and R JONES, Edts.,Nijhoff Publishers, (1983) 243-256.

(1b) ZHENG, C Q and RADON, J C. 'The formation of voids in the ductile fracture of a low alloy steel' in Proc. ICF. Int. Symp. on Fracture Mechanics, Science Press, Beijing, China, (1983) 1052-1056.

(1c) BRANCO, C M, RADON, J C and CULVER, L E 'Elastic-plastic fatigue crack growth under load cycling' J. Strain Analysis, 12 (1977) 71-80.

(1d) RADON, J C. 'Fatigue of low alloy steel BS4360-50D' in Collected Papers on Fracture Research, Part 7, (in Chinese) Northwestern Polytechnical University Press, Xian, (1983).

(2) CHEN CHI, YAO HENG, DENG ZHI-SHANG, ZHUANG TAO and DENG QI-YAUN. 'Interrelation of J-integral and crack tip opening displacement', Collected Papers on Researching Fracture of Metals, (in Chinese), (1978) 64-76.

(3) BRIDGMAN, P W. 'Studies in large plastic flow and fracture', (1952) 9-86.

(4a) DE CASTRO, P M S T, RADON, J C and CULVER, L E. 'J-resistance curve and ductile tearing of a mild steel', Int. J. Fatigue, (1979) 153-158.

(4b) DE CASTRO, P M S T, SPURRIER, J and HANCOCK, P. 'Comparison of J testing techniques and correlation: J-COD using structural steel specimens', Int. J. Fracture, 17 (1981) 83-95.

(5) PISARSKI, H G. 'Influence of thickness on critical crack opening displacement (COD) and J values', Int. J. Fracture, 17 (1981) 427-440.

(6) CHEN CHI. 'The stress analysis in the neck of a tension test specimen', Collected Papers on Researching Fracture of Metals, (in Chinese), (1978) 169-189.

(7) LAUTRIDOU, J C and PINEAU, A. 'Crack initiation and stable crack growth resistance in A508 steels and in relation to inclusion distribution', Engng. Fract. Mechan., 15 (1981) 55-71.

(8) McMEEEKING, R M. 'Finite deformation anlysis of crack tip opening in elastic-plastic materials and implications for fracture', J.Mech. Phys. Solids, 25 (1977) 357-381.

(9a) RADON, J C. 'Toughness changes in gross plasticity cycling', in Non-Linear Problems in Stress Anlysis. ed. P. Stanley, Chapter 3 Applied Science Publishers, London (1978) 41-64.

(9b) WILLOUGHBY, A A, PRATT, P L and TURNER, C E. 'The meaning of elastic-plastic fracture criteria during slow crack growth', Int. J. Fracture, 17 (1981) 449-466.

(10) PARANJEE, S A and BANERJEE, S. 'Interrelation of crack opening displacement and J-integral' , Engng. Fract. Mech, 11 (1979) 43-53.

TABLE 4

Yield stress, σ_y	383 MPa
Ultimate tensile strength, σ_μ	543 MPa
Young's moduls, E	213 GPa
Elongation, A	33%
Reduction in area, Ψ	65.5%

Gauge length = 5.65 $\sqrt{S_o}$, where S_o is the cross-sectional area of the specimen.

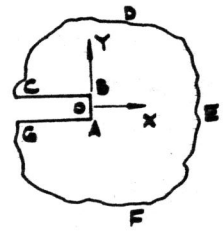

Figure 1 : Crack opening displacement. Schematic

Figure 2 : Crack tip. Schematic

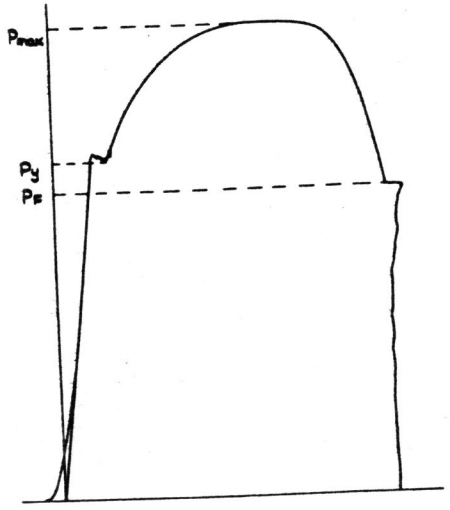

Figure 3 : Steel BS4360-50D. Load-displacement curve. Loading rate 0.0025 in/min at 21°C. Ref. [1a].

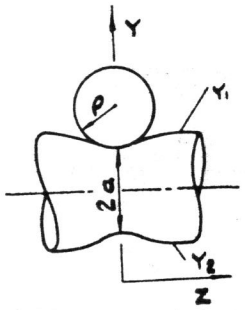

Figure 4 : Necking of a tensile specimen. Schematic.

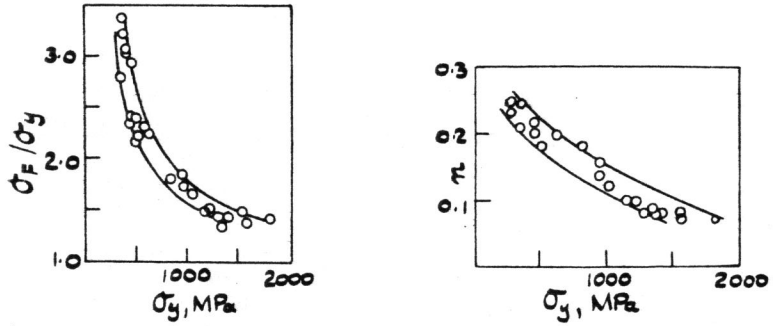

Figure 5 : Mild steels (reference [2])
(a) σ_f/σ_y versus σ_y (b) n versus σ_y

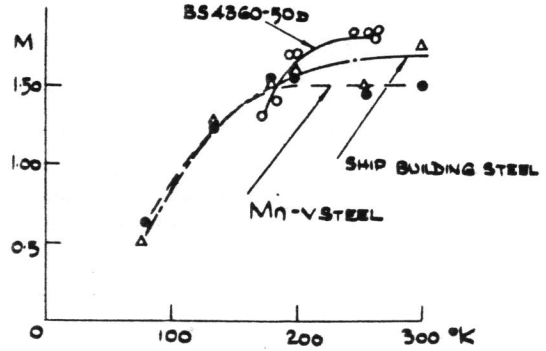

Figure 6 : Variation of M with temperature
Results from three-point bend tests [4,10] and [1b].